Pergamon

Cement and Concrete Research 29 (1999) 933–943

CEMENT AND CONCRETE RESEARCH

Mercury porosimetry of hardened cement pastes

Raymond A. Cook [a,*], Kenneth C. Hover [b]

[a]*Department of Civil Engineering, 236 E Kingsbury Hall, The University of New Hampshire, Durham, New Hampshire 03824, USA*
[b]*Department of Civil and Environmental Engineering, Cornell University, Ithaca, New York 14853, USA*

Manuscript received 9 December 1998; accepted manuscript 22 March 1999

Abstract

Mercury porosimetry was performed on 92 hardened cement paste specimens of water/cement (w/c) ratios 0.3, 0.4, 0.5, 0.6, and 0.7 and curing times of 1, 3, 7, 14, 28, and 56 days. This paper presents the experimental techniques, results, and their possible implications with respect to pore connectivity. As expected, longer curing times and lower w/c ratios resulted in smaller indicated total porosities and smaller threshold pore widths. Longer curing times and higher w/c ratios resulted in greater degrees of hydration. In most of the mercury intrusion results, two peaks could be observed in the differential curves that were identified as the "initial" and "rounded" peaks. The initial peak may correspond to the intrusion of mercury through a connected capillary network, while the rounded peak may correspond to the crushing of interposed hydration products. © 1999 Elsevier Science Ltd. All rights reserved.

Keywords: Mercury porosimetry; Microstructure; Pore size distribution; Permeability; Cement paste

Concrete is a heterogeneous material in which aggregates are held in place by a hardened cement paste binder. The properties of this binder are, therefore, critical to the performance of the concrete as a whole. To better understand the properties of the binder, it is necessary to study the paste microstructure and to see how it is affected by different mixing proportions of water to cement and how the microstructure is affected as the reaction of cement with water proceeds over time. One technique that has been used to study the microstructure of hardened, portland cement pastes is mercury intrusion porosimetry [1–5]. This paper presents the results of 92 porosimetry experiments applied to portland cement pastes of five different water cement (w/c) ratios that were examined at six different curing ages.

1. Methods

1.1. Mercury intrusion porosimetry

With mercury intrusion porosimetry (MIP), porous samples are introduced into a chamber, the chamber is evacuated, the samples are surrounded by mercury, and pressure on the mercury is gradually increased. As the pressure increases, mercury is forced into the pores on the surface of the sample. If the pore system is continuous, a pressure may be achieved at which mercury can penetrate the smallest pore necks of the system and penetrate the bulk sample volume. If the pore system is not continuous, mercury may penetrate the sample volume by breaking through pore walls. By tracking pressures and intrusion volumes during the experiment, it is possible to get a measure of the connecting pore necks of a continuous system or a breakthrough pressure in a discontinuous system. The pore width corresponding to the highest rate of mercury intrusion per change in pressure is known as the "threshold," "critical," or "percolation" pore width. After achieving this highest rate of intrusion, mercury has been shown to penetrate the interior of the sample [3]. Using the technique, one also obtains a measure of the total porosity in the sample as that corresponding to the volume of mercury intruded at the maximum experimental pressure divided by the bulk volume of the unintruded sample.

1.2. Limitations

Because mercury must pass through the narrowest pores connecting the pore network, MIP cannot provide a true pore size distribution [6,7]. The threshold pore width, however, may provide a better indicator of material durability as it has an important influence on the permeability and diffusion characteristics of the cement paste [8]. Total porosity values by mercury porosimetry also differ from those obtained by other techniques. Mercury porosimetry will indicate smaller than actual porosity values where pores are too small or too isolated to be intruded by mercury. On the other hand, MIP porosities may be closer to actual values than

* Corresponding author. Tel.: 603-862-1411; Fax: 603-862-2364; E-mail: ray.cook@unh.edu.

0008-8846/99/$–see front matter © 1999 Elsevier Science Ltd. All rights reserved.
PII: S0008-8846(99)00083-6

those indicated by other techniques where mercury pressures can collapse small pores or break through to isolated pores [9–13].

1.3. Materials

Cement pastes were made from a Type I portland cement and distilled, deaerated water [14].

1.4. Sample preparation and curing

Cement pastes of 0.3, 0.4, 0.5, 0.6, and 0.7 (±0.001) were prepared by adding sifted cement to chilled water in an acrylic canister, sealing the canister, applying a vacuum to the canister, and then shaking the canister in a commercial paint shaking machine for 3 to 8 min [7,14,15]. Unless otherwise noted, uncertainties and error bars correspond to a 95% confidence interval. Paste temperatures ranged from 24.2 to 28.2°C roughly 20 min after mixing was stopped. The pastes were then poured into plastic cylinder molds, 51 × 102 mm size, with elastic latex liners. Liners were used to allow pastes to contract in volume during the first 24 h of curing. The molds were sealed and placed on a rotisserie where they rotated about their longitudinal axis at a rate of 3.2 revolutions per min. A rotisserie was used to minimize possible effects of bleeding and segregation. The rotisserie, in turn, was located in a chamber with a controlled temperature of 23.0 ± 0.1°C.

After being cured for 23.3 to 24.0 h, the hardened paste cylinders were removed from the plastic molds and stored in lime-saturated water at 23.0 ± 1.7°C so that total, nominal, curing periods of 1, 3, 7, 14, 28, and 56 days were achieved, including the 1 day of sealed curing. Herein, pastes are designated by a number where the digits to the left of the decimal point indicate the days of curing and the number to the right of the decimal point indicates the w/c ratio. For example, paste 28.4 was cured for 28 days after being created at a 0.4 w/c ratio. The 3.7 paste was inadvertently cured for 4 days rather than 3 days. The nomenclature, however, is retained for consistency. Other curing periods were within 6% of the nominal value.

1.5. Drying

At the end of each curing period, two slices measuring 13 ± 1 mm were cut from a cylinder using a water-cooled, diamond-bladed, geologic saw and four cubes measuring 13 ± 1 mm per side were cut from the center portion of each slice. These cubes were then weighed in a saturated, surface-dry condition and then placed into a vacuum desiccator for drying.

The drying method employed was a variation on the D-drying method of Copeland and Hayes [16]. As with the method of Copeland and Hayes, the desiccator is evacuated by a vacuum pump through a tubing path exposed to −79°C. The method used here differs from that of Copeland and Hayes in that discrete, relatively large specimens (the sample cubes) were dried, as opposed to Copeland and Hayes' method of drying the samples of particles passing a No. 30 and retained on a No. 80 sieve. The use of large specimens was to obtain the best possible results from mercury porosimetry where individual specimens are preferable to the use of a sample of particles [6,17,18]. The use of a single specimen eliminates the possibility that the intrusion of mercury between the particles of a powder sample will be confused with that corresponding to the porosity of the particles themselves [19–21]. Furthermore, using a single, large specimen in a porosimetry experiment minimizes the surface area to volume ratio of the sample thus minimizing boundary effects. The use of cubes, in turn, resulted in a vacuum of 20 ± 7 Pa (as opposed to 3 ± 1 Pa), and prompted the selection of a more stringent drying end point than that of Copeland and Hayes. Samples were dried for 27 to 29 days and the D-dried weights were taken as those corresponding to a weight loss of 0.01%/day (as opposed to Copeland and Hayes' 0.1%/day [14]).

1.6. Degree of hydration

The degree of hydration, α, is defined as the fraction of cement that has fully hydrated [22,23]. For the present experiments, α was determined experimentally by comparing the amount of nonevaporable water in a sample to the amount needed for complete hydration. To determine the nonevaporable water content, four dried specimens from each paste group were subjected to ignition at 1000 ± 50°C for 1 h, cooled in a vacuum desiccator at less than 20 Pa for 1 h, and then weighed. The water in the paste that was not removed by the drying process, w_n, (also known as the nonevaporable water) is then estimated as shown in Eq. (1) [16,22]

$$\frac{w_n}{c} = \frac{w_1}{w_2}\left(1 - \frac{L}{100\%}\right) - 1 \tag{1}$$

where w_1 and w_2 are the weights of the dry specimen before and after ignition, respectively. The factor $(1 - L/100\%)$ is an adjustment made to compensate for the percent weight loss on ignition, L, of the original cement and is based on the assumption that this loss is the same before and after cement hydration. Given w_n/c, the degree of hydration can then be calculated as shown in Eq. (2):

$$\alpha = \frac{w_n/c}{(w_n/c)^{\circ}} \tag{2}$$

where $(w_n/c)^{\circ}$ is the nonevaporable water corresponding to a completely hydrated paste.

For the present work, the value for L was determined by igniting twelve 3 to 4 g specimens of unhydrated cement and was found to be 1.223 ± 0.024%. The value for P-dried $(w_n/c)^{\circ}$ was estimated as 0.276 ± 0.005 [14] using generally accepted equations [23–25]. Accepting the finding of Copeland and Hayes [16] that the D-drying method removes approximately 1.084 times more water than does the P-drying method used by Powers, the equivalent D-dried $(w_n/c)^{\circ}$

value was taken to be 0.276/1.084 or 0.255 ± 0.005. The 0.255 value is similar to that used by others [26] and was used in Eq. (2) for the estimation of α for the present work.

1.7. Mercury intrusion porosimetry

After drying, the bulk volumes of four sample cubes were measured using a calibrated mercury displacement pycnometry method that yielded an uncertainty of ±0.0039 mL for the approximately 2 mL cubes [14]. After the volume of a cube was measured, the cube was placed in the chamber of an automated porosimeter (a Model PMI 60K-A-2 manufactured by Porous Materials Inc., Ithaca, NY, USA) and the chamber evacuated to 20 Pa. Mercury was then introduced to the chamber, the hydrostatic head of which yielded an initial low pressure of 5 kPa. Pressure was subsequently increased in 55 to 60 pressure increments to a maximum pressure of approximately 300 MPa. These pressure increments were chosen to correspond to even intervals on a logarithmic scale. After each pressure increment, the machine was set to pause and allow the pressure and volume readings to stabilize before recording a pressure/volume data pair. The average time to achieve full pressure during an experiment was approximately 1 h and 45 min. Two replicates were performed on the 1.6 paste, four replicates each for the 56.3, 1.7, and 3.7 pastes, and three replicates each for the other 26 pastes.

1.8. Corrections to porosimetry data

Porosimetry data was processed using software developed by the researchers. In processing the data, certain assumptions and corrections discussed elsewhere [6,27] need to be applied. Pressures were corrected to account for the hydrostatic mercury head above the geometric center of gravity of the specimens and, subsequently, corrected pressures were converted to equivalent pore widths using a modified form of the Washburn equation, as in Eq. (3):

$$d = \frac{-\phi\gamma_\infty\cos\theta}{p} + 4b\cos\theta. \quad (3)$$

Here, d is the pore width, ϕ is a pore shape factor, γ_∞ is the surface tension of mercury for a planar meniscus, θ is the contact angle between mercury and the pore wall, p is the net pressure across the mercury meniscus at the time of the cumulative intrusion measurement, and b is the effective radius of a mercury atom (approximately 270 picometers). The values for ϕ, γ_∞ θ were assumed to be 3, 0.480 N/m, and 130° respectively. Volume measurements were corrected by a blank run for differential mercury compression and for specimen compression (where the compressibility of the specimens was assumed to be 1×10^{-11} m^2/N). Sample cumulative porosities were calculated as the corrected intrusion volume of mercury divided by the bulk volumes of the samples as measured before the experiment by mercury displacement pycnometry.

2. Results

2.1. Degree of hydration

Degrees of hydration vs. time and paste type are given in Fig. 1. With one possible exception, measured degrees of hydration increase with curing time. The apparent exception—the 0.4 w/c paste between 28 and 56 days of curing—may be a result of the uncertainty in the measurements. Degrees of hydration also increased with increasing w/c ratio. All pastes achieved approximately 35% hydration after 1 day of seal curing. After nominally 56 days, hydration ranged from 50.8 ± 2.0% for the 0.3 w/c paste to 81.7 ± 3.2% for the 0.7 w/c paste.

2.2. Mercury intrusion

Porosities measured varied from approximately 16% for the 0.3 paste cured for 56 days to 56% for the 0.7 paste cured for 1 day (Fig. 2). Well-defined threshold pore widths were evident from approximately 2 μm to 20 nm. Reproducibility among the replicates was good and, as expected, increased curing time and decreased w/c ratio resulted in lower total porosities and smaller values of threshold pore width for all pastes.

It was also noted that as pastes cured, the character of the porosimetry curves changed. Differential MIP curves for pastes cured for the least amount of time exhibited a sharply defined initial peak indicating a unimodal distribution of pore sizes. As curing times increased, a second, more rounded peak appeared at smaller pore sizes thus suggesting a bimodal distribution. With increasing curing times, the initial sharp peak became less dominant and, in all but the 0.7 w/c pastes, disappeared altogether. The lower the w/c ratio was, the sooner the initial peak disappeared. The 0.3 w/c paste was unique in that curves did not exhibit two peaks at any curing period tested. Differential curve shapes can be affected by the number of points taken during a porosimetry run. Shapes stabilize as the number of points taken

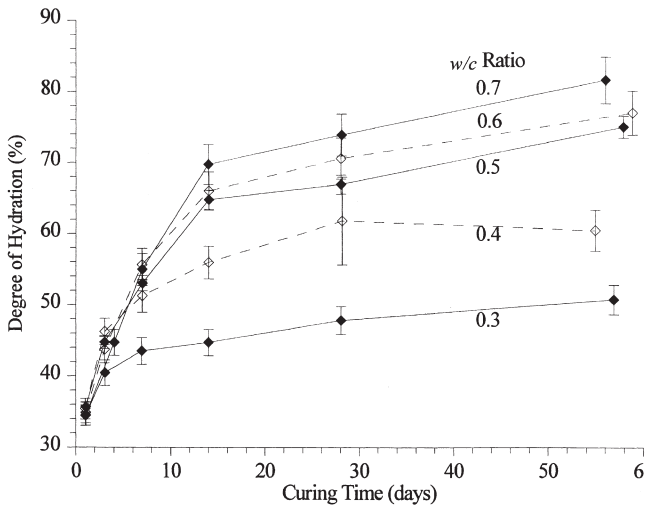

Fig. 1. Degree of hydration, α, as a function of curing time.

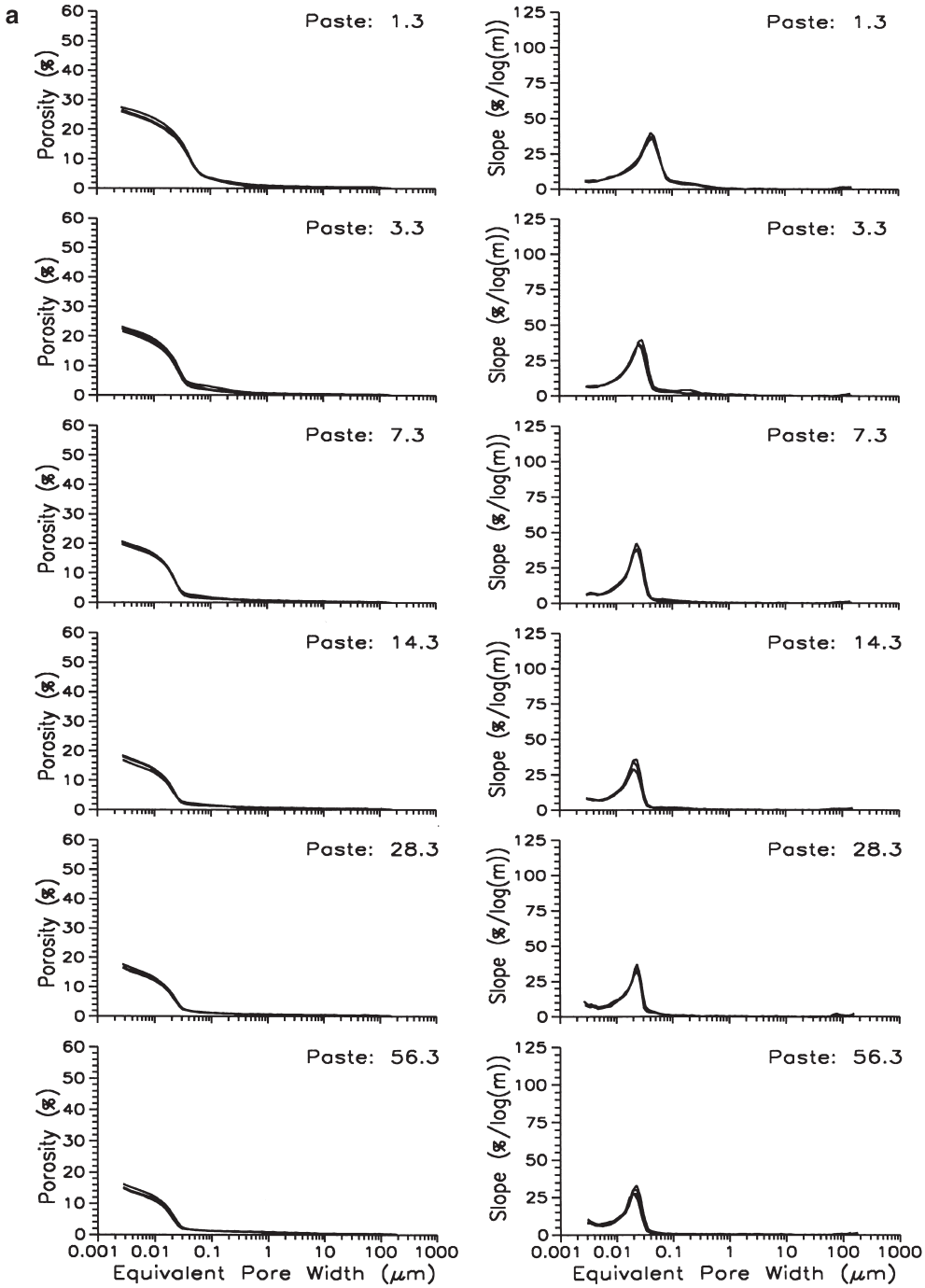

Fig. 2. Results from mercury intrusion into pastes made with a w/c ratio of *(a)* 0.3, *(b)* 0.4, *(c)* 0.5, *(d)* 0.6, *(e)* 0.7.

increases. The number of points selected for these runs was based on the researchers' experience as being sufficient to achieve stable and reproducible differential curves.

With respect to reproducibility among the replicates, the maximum difference between the greatest and least total porosity values for a given paste group was 4.0% with an average difference of 1.9% and an average standard error of the resultant mean of 0.6%. Threshold pore widths varied more. With one exception, the maximum difference between the maximum and minimum value was 56% with an average difference of 17% and an average standard error of the mean of 5.3%. The exception was a 126% difference exhibited by the 14.5 paste.

As expected, increased curing time and decreased w/c ratio results in lower total porosities and smaller values of threshold pore width for all pastes (Figs. 3, 4, 5, and 6). The minimum values of total porosity and threshold pore width were obtained by minimizing w/c ratio and maximizing curing time. Experimental results for pastes with increasing w/c ratio and partially compensating increases in curing

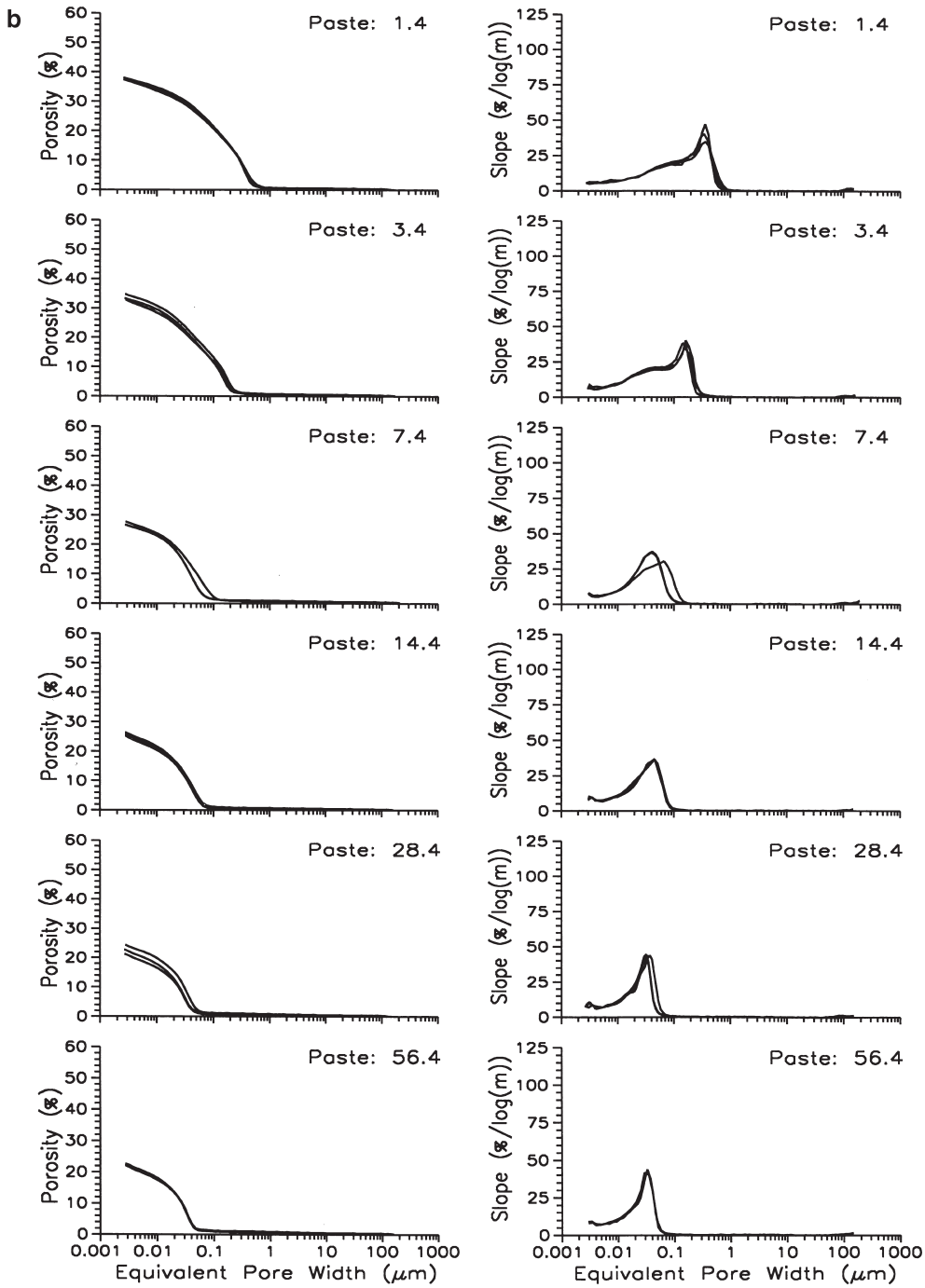

Fig. 2. *(continued).*

time are given in Fig. 7. For the paste specimens investigated, lowering the w/c ratio by 0.1 is more effective at minimizing threshold pore widths and total porosities than is doubling the curing period.

3. Discussion

Experimental reproducibility was good. The variation in total porosity (less than 4.0%) compares favorably with the less than 6% found by Hearn and Hooton [21]. It is widely accepted that as hydration proceeds, hydration products grow into the pore space of a hardened cement paste. Therefore, that increased curing time and decreased w/c ratio result in lower total porosity values and smaller threshold pore widths was expected and agrees with the data of others [1,3,4,28,29].

A careful inspection of the data of others also provides indications of the existence of initial and rounded peaks

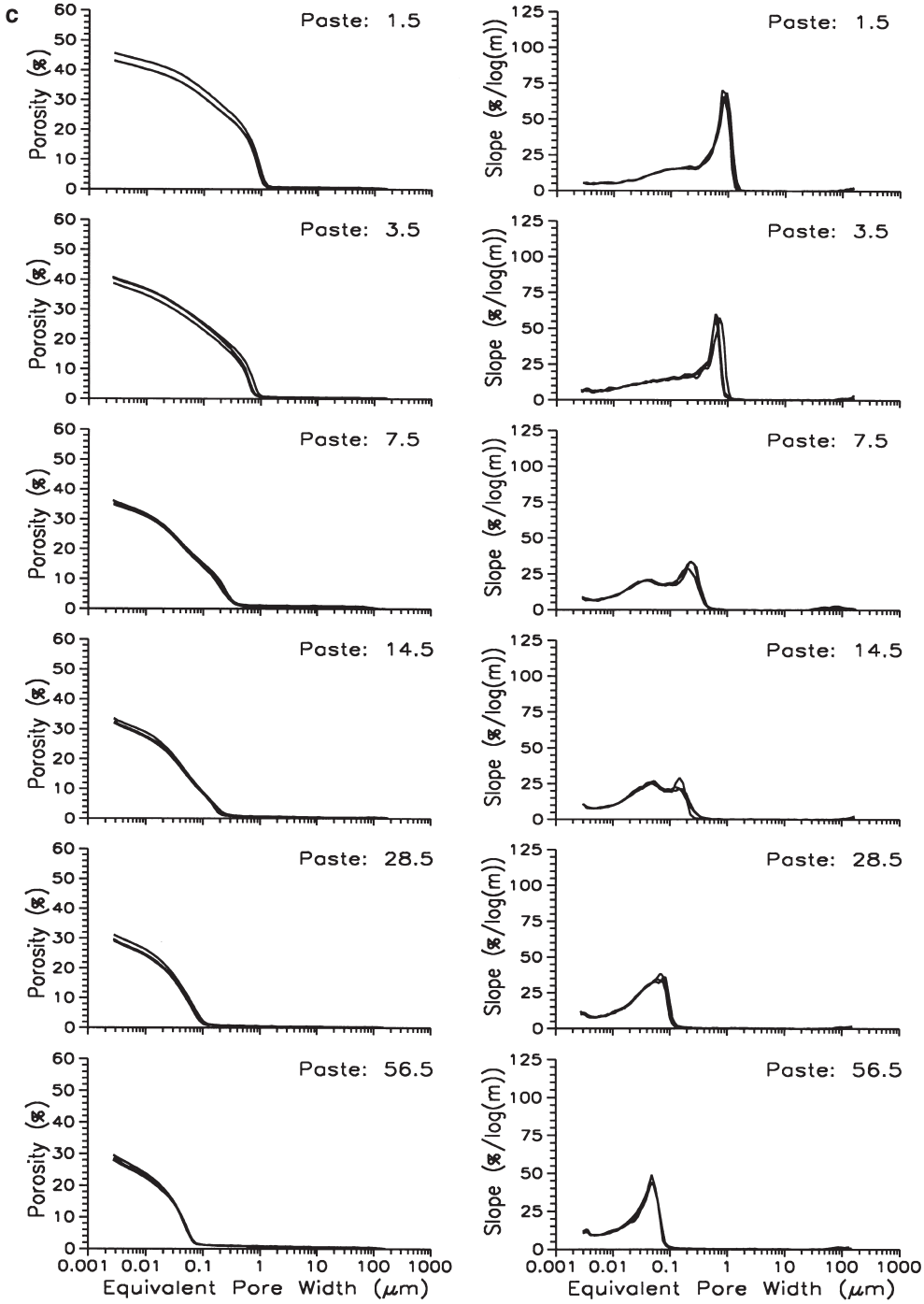

Fig. 2. *(continued)*.

[3,5,28,30–34]. The presence of a sharply defined intrusion peak in the differential curve indicates the intrusion of mercury throughout the specimen through a pore network connected to the specimen surface [3,8,30,35]. It appears, therefore, that the initial intrusion peak observed here corresponds to the minimum throat dimension of an interconnected capillary network. As hydration proceeds and hydration products expand into the pore space, it is logical that the size of connecting pores would diminish. This corresponds to the experimentally observed movement of the initial peak to smaller pore widths.

The appearance and growth of the rounded peak, however, may indicate a different intrusion mechanism. One possibility is that the rounded peaks correspond to intrusion into a material phase with a distinct network of smaller pores. The roundness of the peak would then correspond to a wide distribution in pore sizes for this material phase. That the rounded peaks become more dominant as hydration pro-

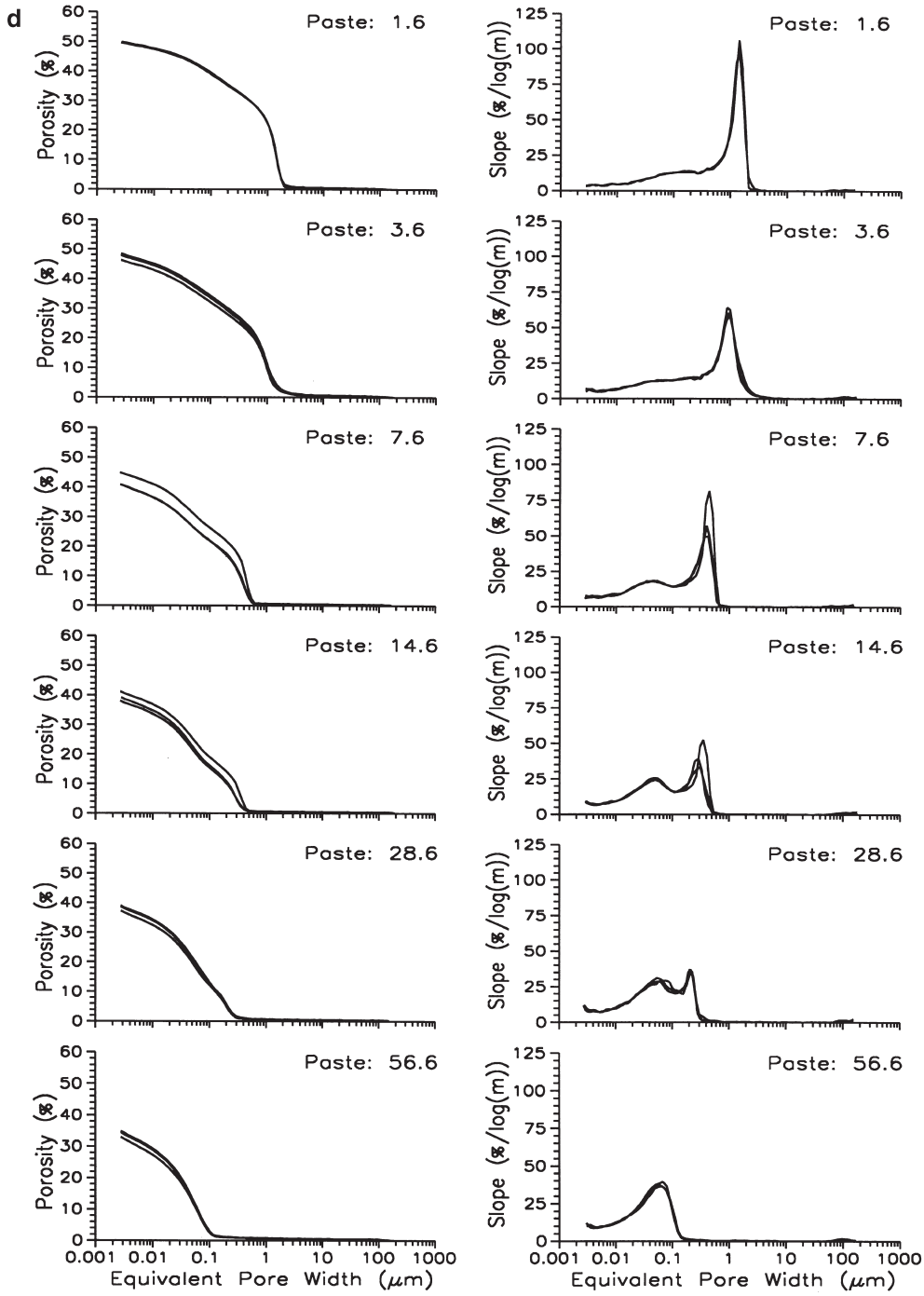

Fig. 2. *(continued)*.

ceeds would indicate that the volume of this material phase is increasing with increased hydration. Such a phenomenon would correspond to the appearance of the "gel" porosity of the Powers model. However, the experimental results do not agree with the Powers model or with data from adsorption studies because the pore sizes of the rounded peaks seen here (between 20 to 60 nm) is far larger than the 1 to 2 nm expected for gel pores.

Recalling that pore sizes are inferred from intrusion pressures, there is another explanation of the source of the rounded peak. It is possible that the rounded peak corresponds not to a pore size, but rather to the crushing strength of hydration products impeding the intrusion of mercury. During the course of hydration, it is possible that clear interconnections between pores become entirely blocked. This would correspond to the observed disappearance of the initial intrusion peak. If pore volume still exists but is isolated, mercury may be able to either intrude through or break open

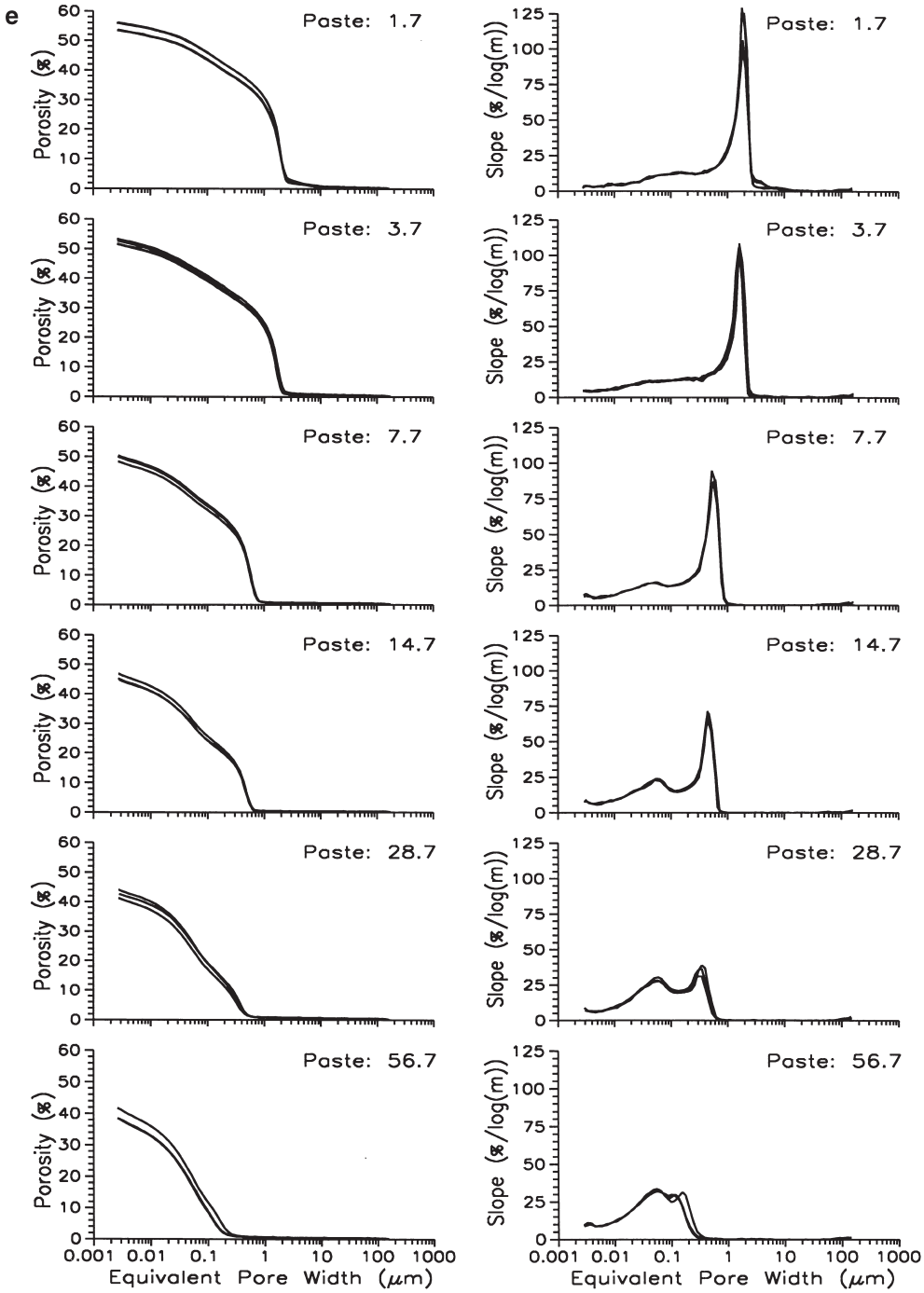

Fig. 2. *(continued)*.

the blockages during the course of the experiment. If this is the case, the rounded peak corresponds not to a width of interconnected pores, but to either a characteristic pore width associated with the blocking hydration products or the crushing pressure of the interposed products.

Again, the pore widths measured here are larger than we would expect in blocking hydration products. On the other hand, if the second peak corresponds to a crushing mechanism and if the gel products are fairly uniform regardless of the initial w/c ratio and curing time, the indicated crushing strength of the gel should also be roughly uniform. This would explain why the rounded peaks are relatively stable with respect to the pore width axis. While initial intrusion peaks move from 2 μm to less than 200 nm (an order of magnitude), the rounded peaks are all within a range of 20 to 60 nm. That the peaks are more rounded than the initial intrusion peaks also is logical as barriers can be expected to vary in strength depending on the size of the space between

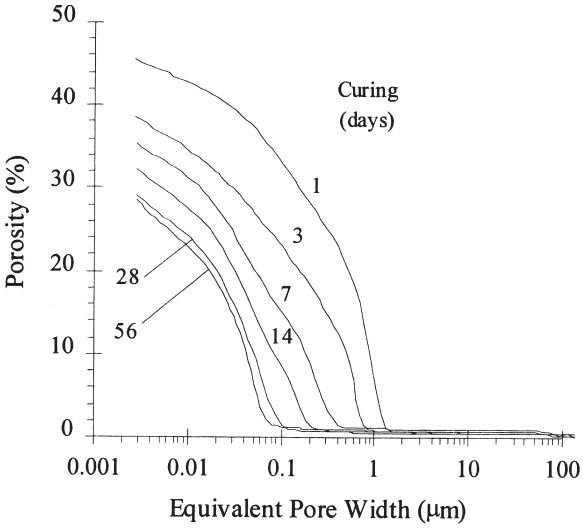

Fig. 3. The effect of curing on MIP results for pastes of w/c = 0.5.

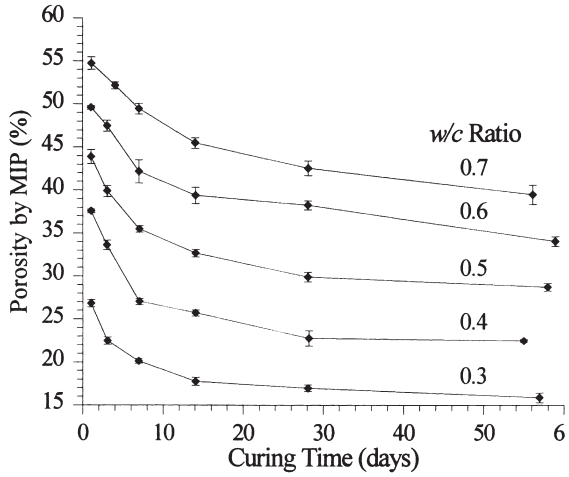

Fig. 5. Summary of the effect of curing time and w/c ratio on total porosity as determined by MIP.

unhydrated cement grains and depending on the thickness of the barriers. If this hypothesis is correct, the crushing strength of cement gel barriers is between 15 and 45 MPa (2200 to 6600 psi). Furthermore, the greater of these crushing strengths corresponds to the low w/c pastes that also have smaller distances between unhydrated cement grains. That both peaks exist in pastes of intermediate curing age may correspond to the coexistence of interconnected capillary pores and regions of capillary pore space blocked from the exterior by gel barriers. In the 0.3 w/c ratio pastes, no initial intrusion peak is observed. It may be that in these pastes, sufficient hydration products have formed after only one day to isolate the interior pore space.

Additional corroboration of the hypothesis that capillary pores become discontinuous can be found in the discussion of permeability by Powers et al.[36] and in an investigation of capillary pore percolation by Bentz and Garboczi [37,38]. Both teams of investigators concluded that at certain degrees of hydration, the capillary pore network becomes discontinuous. Powers et al. summarized their results in a figure in which, given a w/c ratio, the degree of hydration at which the capillary pores becomes discontinuous can be estimated. Bentz and Garboczi concluded that capillary pores become discontinuous when the capillary porosity is 18% or less, regardless of the w/c ratio or degree of hydration required to achieve the 18% value.

The curve from the figure of Powers, Copeland, and Mann has been reproduced in Fig. 8 with a line corresponding to Bentz and Gaboczi's 18% porosity [14,37]. Additionally, vertical bars have been added that correspond to the degrees of hydration at which the initial intrusion peak disappeared from the data presented in Part I of this paper.

For plotting experimental MIP data, bars are used rather than points because it is uncertain as to the precise degree of hydration corresponding to the disappearance of the initial intrusion peaks. For example, the initial peak disappears from the 0.6 w/c data between 28 and 56 days or between

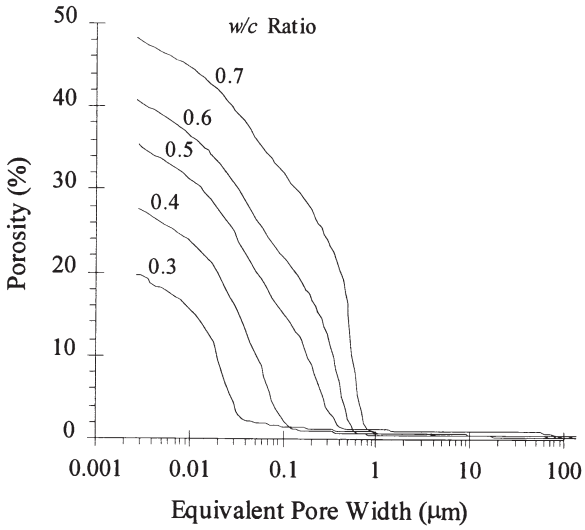

Fig. 4. The effect of w/c ratio on MIP results for pastes cured for 7 days.

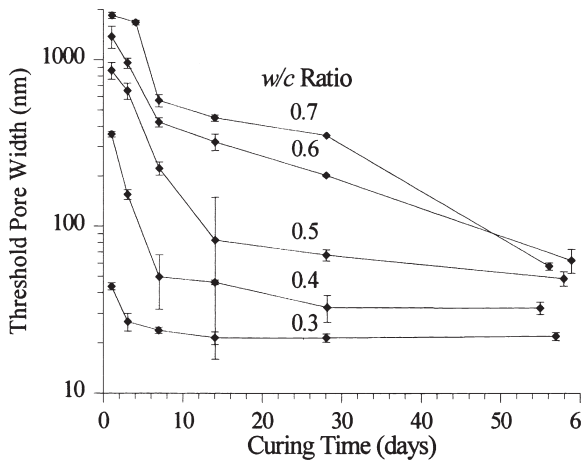

Fig. 6. Summary of the effect of curing time and w/c ratio on threshold pore width as determined by MIP.

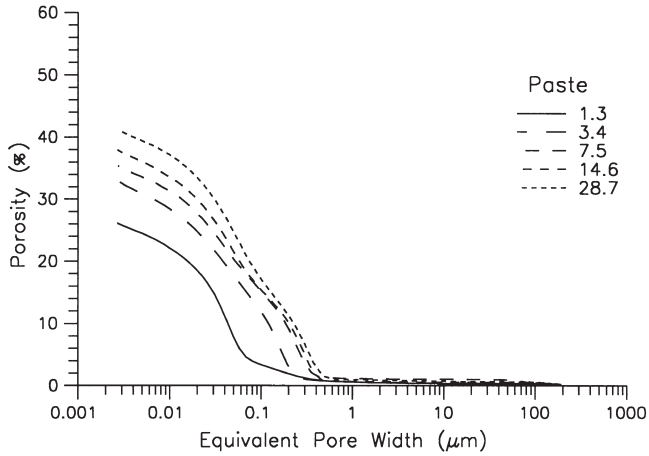

Fig. 7. Contrasting effects of increasing w/c ratio with increasing curing time on MIP results.

corresponding degrees of hydration of 70 and 77%. Thus, the peak could have disappeared at any degree of hydration within this range and a corresponding bar from 70 to 77% is plotted. For the 0.3 paste the peak has already disappeared by the time α has reached 35% ,and for the 0.7 paste the peak has not yet disappeared by the time α has reached 82%. Hence, for these pastes bars proceed to the limits of the figure. The slope of the 18% porosity line is similar to both the Powers et al. curve and the experimental results. For a given w/c ratio, however, the 18% porosity line yields a degree of hydration approximately 20% higher than that indicated by the experimental results. In other words, the experimental results from this study indicate that capillary pores become discontinuous earlier in the curing period than indicated by the findings of Bentz and Garboczi. If the disappearance of the initial intrusion peak does correspond to a discontinuous pore system, the experimental data indicate that pores become discontinuous at an MIP porosity of between 28 and 35%.

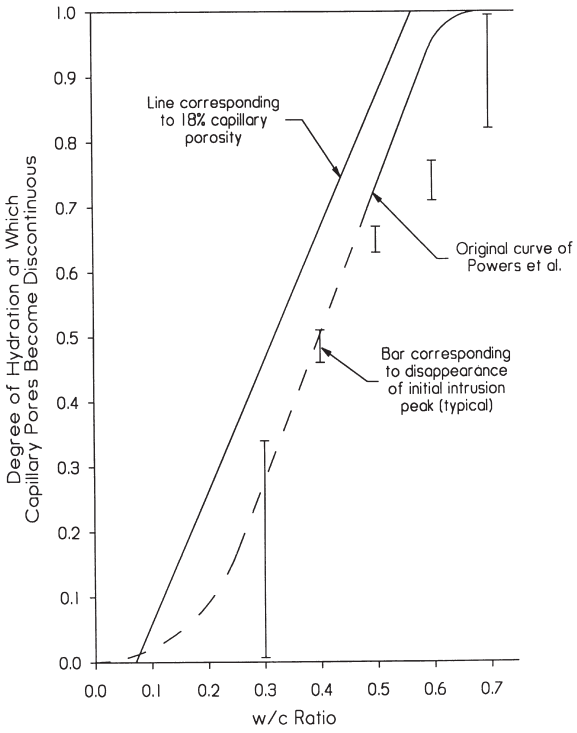

Fig. 8. A comparison between the w/c ratio and the degree of hydration at which capillary pores become discontinuous according to Powers et al. [36] (dashed and solid curves) and the degrees of hydration at within which the initial intrusion peak disappeared from the present research (vertical bars).

The Powers et al. curve is based on two experimentally determined points and estimates for others. Considering that the curve corresponds to pastes made from a different cement, there is good agreement between their data and the present theory that the disappearance of the initial peak corresponds to a state of discontinuous capillary pores.

4. Conclusions

1. Degrees of hydration were achieved from 35 to 82% depending on water cement ratio and curing time. Longer curing times and higher w/c ratios resulted in greater degrees of hydration.
2. Porosity as measured by mercury intrusion varied from 16 to 56% depending on w/c ratio and curing time. Longer curing times and lower water cement ratios resulted in lower porosity values.
3. Threshold pore widths varied from 2 μm to 20 nm. Longer curing times and lower water cement ratios resulted in lower threshold pore width values.
4. For the paste specimens investigated, lowering the w/c ratio by 0.1 is more effective at minimizing threshold pore widths and total MIP porosities than doubling the curing period is.
5. As pastes cure, the character of the porosimetry curves changes. Differential MIP curves exhibit two types of peaks: a sharp initial peak and a rounded peak. The initial peak shifts to smaller pore sizes and diminishes in size with increased curing time and lower w/c ratios. The rounded peak does not shift as much and becomes more dominant with increased curing time and lower water cement ratios.
6. The initial peak exhibited in differential MIP curves of hardened cement paste appears to correspond to the size of pore necks connecting a continuous capillary pore network, disappearing as pores become blocked with hydration product.
7. The rounded peak exhibited in differential MIP curves of hardened cement paste appears to correspond to the pressure required to break through blockages in the capillary pore network.

References

[1] U. Ludwig, H.E. Schwiete, Porosity measurements of cement pastes, cement mortars, and concretes, Proc. 8th Conf. Silicate Industry, F. Tamas (ed.), Budapest, 1966, pp. 235–251.

[2] G.J. Verbeck, R.H. Helmuth, Structures and physical properties of cement paste, Proc. 5th International Symp. Chem. Cem., Vol. 3, Tokyo, 1968, pp. 1–32.
[3] D.N. Winslow, S. Diamond, A mercury porosimetry study of the evolution of porosity in cement, ASTM J. Materials 5 (3) (1970) 564–585.
[4] N.McN. Alford, A.A. Rahman, An assessment of porosity and pore sizes in hardened cement pastes, J Materials Science 16 (1981) 3105–3114.
[5] H.G. Midgley, J.M. Illston, Some comments on the microstructure of hardened cement pastes, Cem Concr Res 13 (1983) 197–206.
[6] R.A. Cook, Fundamentals of mercury intrusion porosimetry and its application to concrete materials science, Master of Science Thesis, Cornell University, 1991.
[7] S. Diamond, D. Bonen, Microstructure of hardened cement paste—A new interpretation, J Amer Cer Soc 76 (12) (1993) 2993–2999.
[8] E.J. Garboczi, Permeability, diffusivity, and microstructural parameters: A critical review, Cem Concr Res 20 (1990) 591–601.
[9] S. Diamond, A critical comparison of mercury porosimetry and capillary condensation pore size distributions of portland cement pastes, Cem Concr Res 1 (1971) 531–545.
[10] J.J. Beaudoin, Porosity measurement of some hydrated cementitious systems by high pressure mercury intrusion: Microstructural limitations, Cem Concr Res 9 (1979) 771–781.
[11] H. Cheng-yi, R.F. Feldman, Influence of silica fume on the microstructural development in cement mortars, Cem Concr Res 15 (1985) 285–294.
[12] I. Odler, H. Köster, Investigations on the structure of fully hydrated portland cement and tricalcium silicate pastes: II. Total porosity and pore size distributions, Cem Concr Res 16 (6) (1986) 893–901.
[13] P. Gu, P. Xie, J.J. Beaudoin, Microstructural characterization of the transition zone in cement systems by means of A.C. impedance spectroscopy, Cem Concr Res 23 (1993) 581–591.
[14] R.A. Cook, A generalized form of the powers model of cement microstructure and its evaluation via mercury porosimetry and related techniques, Ph.D. dissertation, Cornell University, 1992.
[15] D.N. Winslow, D. Liu, The pore structure of paste in concrete, Cem Concr Res 20 (2) (1990) 227–235.
[16] L.E. Copeland, J.C. Hayes, Determination of non-evaporable water in hardened portland-cement paste, ASTM Bull 194 (1953) 70–74.
[17] D.C. Kopaska-Merkel, Capillary-pressure analysis of small fragments (geological), The MicroReport, Norcross, GA: Micromeritics Corp., Vol. 1, No. 2, 1990, pp. 5–6.
[18] F. Metz, D. Knöfel, Systematic mercury porosimetry investigations on sandstones, Materials and Structures 25 (1992) 127–136.
[19] H.K. Palmer, R.C. Rowe, The application of mercury porosimetry to porous polymer powders, Powder Technology 9 (1974) 181–186.
[20] D.M. Smith, S. Schentrup, Mercury porosimetry of fine particles: Particle interaction and compression effects, Powder Technology 49 (1987) 241–247.
[21] N. Hearn, R.D. Hooton, Sample mass and dimension effects on mercury intrusion porosimetry results, Cem Concr Res 22 (5) (1992) 970–980.
[22] T.C. Powers, The air requirement of frost-resistant concrete, Proc Highway Res Board 29 (1949) 184–211.
[23] S. Mindess, J.F. Young, Concrete, Prentice-Hall, Inc., Englewood Cliffs, NJ, 1981.
[24] A.M. Neville, Properties of Concrete, 3rd ed., Pitman Books Ltd., London, 1981.
[25] P.K. Mehta, Concrete: Structure, Properties, and Materials, Prentice-Hall, Inc., Englewood Cliffs, NJ, 1986.
[26] K.O. Kjellsen, R.J. Detwiler, O.E. Gjørv, Development of microstructures in plain cement pastes hydrated at different temperatures, Cem Concr Res 21 (1) (1991) 179–189.
[27] R.A. Cook, K.C. Hover, Mercury porosimetry of cement-based materials and associated correction factors, ACI Materials J 90 (2) (1993) 152–161.
[28] A.A. Auskern, W. Horn, Capillary porosity in hardened cement paste, J Testing and Evaluation 1 (1) (1973) 74–79.
[29] A. Bentur, The pore structure of hydrated cementitious compounds of different chemical composition, J Amer Cer Soc 63 (7–8) (1980) 381–386.
[30] Ö.Z. Cebeci, Pore structure of air-entrained hardened cement paste, Cem Concr Res 11 (1981) 257–265.
[31] I. Odler, M. Röβler, Investigations on the relationship between porosity, structure, and strength of hydrated portland cement pastes. II. Effect of pore structure and of degree of hydration, Cem Concr Res 15 (1985) 401–410.
[32] H.W. Reinhardt, K. Gaber, Equivalent pore size characterizing the pore size distribution of cement mortar, in: Sidney Mindess (Ed.), Ceramic Transactions: Advances in Cementitious Materials, The American Ceramic Society, Westerville, OH, 1990, pp. 319–335.
[33] C. Lobo, M. Cohen, Pore structure development in type K expansive cement pastes, Cem Concr Res 21 (2/3) (1991) 229–241.
[34] P. Gu, P. Xie, J.J. Beaudoin, R. Brousseau, A.C. impedance spectroscopy: II. Microstructural characterization of hydrating cement-silica fume systems, Cem Concr Res 23 (1) (1993) 157–168.
[35] K.A. Snyder, D.N. Winslow, D.P. Bentz, E.J. Garboczi, Interfacial zone percolation in cement-aggregate composites, RILEM Proceedings, Toulouse, France, 1992.
[36] T.C. Powers, L.E. Copeland, H.M. Mann, Capillary continuity or discontinuity in cement pastes, J. Portland Cem. Assoc. Res. Devel. Labs., May 1959, pp. 38–48.
[37] D.P. Bentz, E.J. Garboczi, Percolation of the phases in a three-dimensional cement paste microstructural model, Cem Concr Res 21 (2/3) (1991) 325–344.
[38] E.J. Garboczi, Computational materials science of cement-based materials, Materials and Structures 26 (1993) 191–195.